

# 1 Entropy Driven Phase Separation

Richard Vink

Institut für Physik  
Johannes Gutenberg-Universität  
Mainz (Germany)

**Abstract.** A grand canonical Monte Carlo method for the simulation of a simple colloid-polymer mixture called the AO model will be described. The phase separation known to occur in this model is driven by entropy. The phase diagram of the unmixing transition, the surface tension and the critical point will be determined.

## 1.1 Introduction

Mixtures of particles are all around us. If you pour oil and water together you create a mixture. Another example is a solution containing colloids and polymers. Mixtures will sometimes phase separate or unmix. When this happens particles of the same kind cluster together. A famous example is a mixture of oil and water: after unmixing, the lower part of the container contains mostly water and the upper part mostly oil with an interface in between.

There are different reasons for a mixture to unmix. For instance, the unmixed state might carry a lower energy. As an example consider a mixture of A and B particles interacting with the following pair potentials:

$$u_{AA}(r) = u_{BB}(r) = 0; \quad u_{AB}(r) = -\frac{a}{r}; \quad (1.1)$$

where  $r$  is the distance between two particles and  $a$  some positive constant. In this mixture, A particles do not feel each other, and neither do B particles, but when A and B particles are close together there is an energy penalty. At low temperature, the system tries to minimize the energy and can only do so by moving the A and B particles as far apart as possible. The system thus unmixes.

There is another mechanism that can induce unmixing. This mechanism has its origin in entropy and not in energy. The unmixing of colloid-polymer mixtures for example is driven by entropy. To show that this must be the case, it is instructive to briefly consider the nature of the interactions in a typical colloid-polymer mixture. To a crude approximation the colloids behave as hard spheres. The polymer interactions are more complicated. A real polymer consists of a chain of bonded monomers. In principle all monomers should be taken into account explicitly. However, under certain conditions it is reasonable to describe the polymer chain with only the coordinate of its center of mass and some effective radius called the radius of gyration. In 1954 Asakura and Osawa [1] proposed a simple model for colloid-polymer

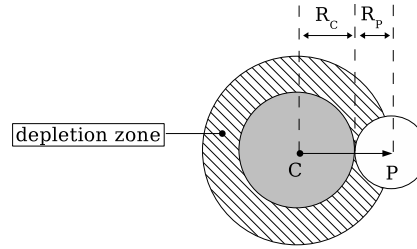


Fig.1.1.1. Colloid and polymer at minimum separation (here and throughout this text  $C$  = colloid and  $P$  = polymer). The distance between the centers of mass equals  $R_c + R_p$ . This is the minimum allowed separation: any smaller separation is punished with infinite energy. The colloid thus carries a spherical depletion zone with volume  $V$  around its center of mass which cannot contain any polymer centers.

mixtures based on precisely these approximations. In this model colloids and polymers are treated as spheres with respective radii  $R_c$  and  $R_p$ . Hard sphere interactions are assumed between colloid-colloid (cc) and colloid-polymer (cp) pairs while polymer-polymer (pp) pairs can interpenetrate freely. This leads to the following pair potentials:

$$\begin{aligned} u_{cc}(r) &= \begin{cases} 1 & \text{for } r < 2R_c \\ 0 & \text{otherwise,} \end{cases} & u_{cp}(r) &= \begin{cases} 1 & \text{for } r < R_c + R_p \\ 0 & \text{otherwise,} \end{cases} & (1.2) \\ u_{pp}(r) &= 0; \end{aligned}$$

with  $r$  again the distance between two particles. The above equations define what is nowadays called the AO model. Note that in 1976 the same model was proposed again and independently by Vrij [2].

According to Eq.(1.2) the energy of a valid AO mixture is always zero. Therefore, if unmixing occurs (and it does) it cannot be explained in terms of the energy argument used before. The reason for unmixing is a little more subtle, see Fig.1.1 and Fig.1.2. Shown in Fig.1.1 is one colloidal particle just touching one polymer. When the particles touch, the distance between the centers of mass equals  $R_c + R_p$ . This is the minimum allowed separation between the particles because any smaller separation carries an infinite energy penalty. In the AO model every colloid is thus surrounded by a region which cannot contain any polymer centers of mass. This region is called the depletion zone. In three dimensions the volume of the depletion zone equals:

$$V = \frac{4}{3} (R_c + R_p)^3; \quad (1.3)$$

Consider now Fig.1.2 which shows a container of volume  $V$  holding zero, one and two colloidal particles. Shown at the top is a polymer which we want to insert into the container. If the container is empty we can place the polymer anywhere so the free volume  $f$  available to the polymer is simply

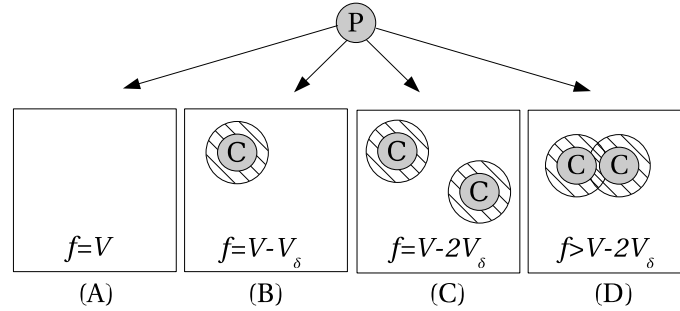


Fig.1.2. Free volume  $f$  available to a single polymer in a container of volume  $V$  holding zero, one and two colloidal particles. See text for details.

$f = V$  (Fig.1.2A). If the container already holds one colloid the free volume decreases to  $f = V - V_\delta$  (Fig.1.2B). The physics becomes interesting when the container holds two or more colloids. Two cases can now be distinguished. In the first case both colloids are well separated and the free volume equals  $f = V - 2V_\delta$  (Fig.1.2C). In the second case the colloids are so close together that their depletion zones overlap and the free volume increases  $f > V - 2V_\delta$  (Fig.1.2D). This immediately has physical consequences: by clustering together the colloids can increase the free volume available to the polymers and hence the entropy of the polymers. Under certain conditions the gain in entropy is sufficient to drive unmixing.

The AO model thus provides a convenient framework in which to study entropy driven unmixing. It has sparked much theoretical work and many simulations [3-7]. Despite its apparent simplicity, predicting the phase behavior of the AO model is no easy task. In this paper an efficient grand canonical Monte Carlo (MC) method that can be used to simulate the AO model will be described. The use of the grand canonical ensemble allows one to bypass certain problems encountered for example in the canonical and Gibbs ensembles. In particular, one can accurately obtain the surface tension and also perform simulations close to the critical point. The method will be used to calculate the phase diagram and the surface tension of the interface. We will also present an accurate determination of the critical point using finite-size scaling.

## 1.2 Grand Canonical Monte Carlo

Imagine an AO mixture contained in some volume  $V$  at inverse temperature  $\beta = 1/(k_B T)$ . In the grand canonical ensemble  $V$  and  $\beta$  are fixed but the number of particles inside  $V$  is allowed to fluctuate. The probability of

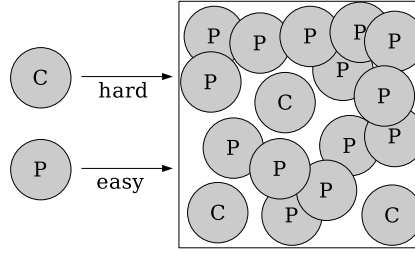


Fig.1.3. Problem encountered in a standard grand canonical MC simulation of the AO model. When the number of polymers in the volume is substantial it becomes difficult to insert additional colloids. Inserting more polymers remains easy though.

observing a volume containing  $N_c$  colloids and  $N_p$  polymers is given by the grand canonical distribution:

$$P = C z_c^{N_c} z_p^{N_p} e^{-E}; \quad (1.4)$$

where  $C$  is a normalization constant,  $E$  the energy given by Eq.(1.2) and  $fz_c; z_p$  the fugacities of the colloids and polymers, respectively.

In a grand canonical MC simulation of the AO model one would like to generate configurations of colloids and polymers that sample Eq.(1.4). In the standard approach this is done by attempting to insert a single particle into  $V$  at a random location, or remove a single (randomly selected) particle from  $V$ . Insertion and removal are usually attempted with equal probability and accepted with probabilities that depend on the energy change of the attempted move and on the fugacities. The standard approach is however not efficient for the AO model as Fig.1.3 illustrates. The figure shows a volume containing a substantial number of polymers and some colloids. According to Eq.(1.2) polymers do not interact with each other so they are happy to overlap. This is what generally will happen as the figure shows. Unfortunately, it is nearly impossible to insert an additional colloid into this system: no matter where the colloid is placed it will likely overlap with at least some of the polymers, and colloid-polymer overlaps are forbidden by Eq.(1.2). A standard grand canonical MC simulation of the AO model is thus characterized by a very low acceptance rate of colloid insertions.

The problem illustrated in Fig.1.3 is typical of asymmetric binary mixtures of which the AO model is an example. The standard grand canonical MC algorithm does not deal well with such mixtures, essentially because it moves only one particle at a time. A MC move capable of removing entire clusters of polymers would be much more efficient. By using such a cluster move the formation of "holes" in the "sea" of polymers is enhanced. If the holes are large enough to contain a colloid, the acceptance rate of colloid insertions will increase. The MC move used in this work to simulate the AO model is aimed at doing precisely that.

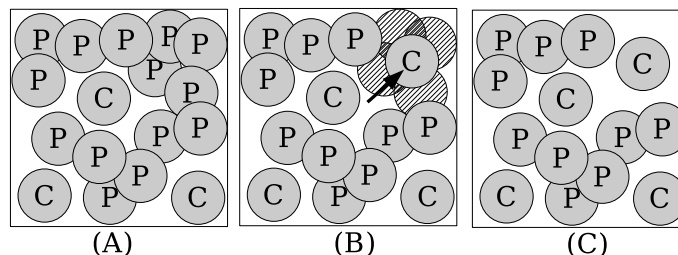


Fig.1.4. Inserting an additional colloid into an AO mixture. (A) The starting configuration. (B) The colloid is inserted at a random location inside the volume. (C) All polymers that overlap with the colloid are removed.

### 1.3 Cluster Moves

Consider now Fig.1.4A which again shows an AO mixture of colloids and polymers. This time we are less shy and simply insert an additional colloid at some randomly selected location inside  $V$ . The resulting configuration is shown in Fig.1.4B, with the colloid inserted in the upper right corner of the box. Note that the configuration in Fig.1.4B is not a valid AO configuration because the colloid overlaps with four polymers. To fix this the overlapping polymers are simply removed, leading to the configuration shown in Fig.1.4C.

The MC move of Fig.1.4 is of course not sufficient to carry out a simulation. We also need a reverse MC move capable of bringing us back from the configuration of Fig.1.4C to the starting configuration of Fig.1.4A. In constructing the reverse move, the key idea is that for every colloid you take out, a number of polymers must be inserted into the empty depletion zone left behind by the colloid. But exactly how many polymers?

To answer this question it is instructive to consider an AO model containing only polymers. In this case the AO model reduces to a very simple system, namely that of an ideal gas (remember that the polymers do not interact with each other). According to basic statistical mechanics, the average density of an ideal gas is equal to its fugacity. Likewise, for an AO model free of colloids, the average polymer density equals  $z_p$ . If we attempt to insert a colloid into the pure polymer system it will on average overlap with  $z_p V$  polymers with fluctuations in the average that are Poisson like, i.e. of order  $\sqrt{z_p V}$ . Because of these fluctuations, the number of polymers  $n_p$  that we must insert for every colloid that we take out cannot simply be a constant. Instead,  $n_p$  must be a random variable drawn from some probability distribution. One choice that works well (see Section 1.6) is to draw it uniformly from the interval  $n_p \in [0; m]$  (so including 0 but excluding  $m$ ) and  $m$  an integer given by:

$$m = 1 + \max_{1 \leq i \leq h} \left\lfloor \frac{z_p V}{z_p V} \right\rfloor; \quad (1.5)$$

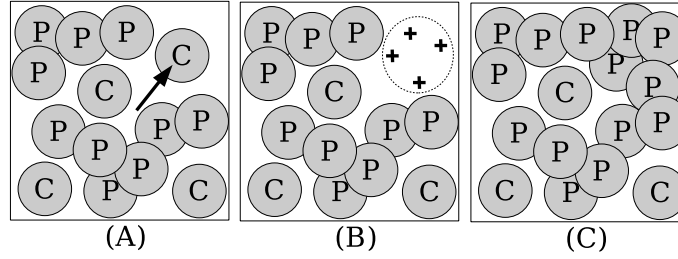


Fig.1.5. MC move used to remove a colloid from an AO mixture. (A) The colloid to be removed is chosen randomly from among those present. (B) The colloid is removed and  $n_p$  random locations are selected inside the empty depletion zone left behind. The number  $n_p$  is uniformly drawn from the interval  $[0; m]$ . In this example  $n_p = 4$ . (C) Polymers are placed onto the random locations.

with a positive constant of order unity you are free to choose (2.0 usually gives good results). Recall that  $V$  is the volume of the depletion zone given by Eq.(1.3).

The reverse move can now be constructed and is illustrated in Fig.1.5. First, we randomly select a colloid (Fig.1.5A). The colloid is removed and  $n_p$  random locations inside the depletion zone of this colloid are selected, with  $n_p$  uniformly drawn from the interval  $[0; m]$  (Fig.1.5B). Finally, polymers are placed onto these random locations resulting in the configuration shown in Fig.1.5C.

#### 1.4 Detailed Balance

We will now derive the acceptance rates of the MC moves illustrated in Fig.1.4 and Fig.1.5. The acceptance rates must be constructed such that detailed balance is obeyed. This is vital because the algorithm must sample the grand canonical distribution of Eq.(1.4). Recall that the condition of detailed balance demands that [8,10]:

$$P(\alpha)g(\beta|\alpha)A(\alpha|\beta) = P(\beta)g(\alpha|\beta)A(\beta|\alpha); \quad (1.6)$$

with  $P(\alpha)$  the Boltzmann probability of state  $\alpha$ ,  $g(\beta|\alpha)$  the probability that the MC scheme generates state  $\beta$  from state  $\alpha$ , and  $A(\alpha|\beta)$  the probability of accepting the new state  $\alpha$ .

The derivation that follows is based on two assumptions:

1. The integer  $m$  of Eq.(1.5) is assumed a constant parameter of the algorithm. It must be set once at the start of the simulation and it may not be changed during the course of the simulation.
2. It is assumed that the insertion of a colloid and the removal of a colloid are attempted with equal probability.

In an implementation it is important that the above conditions are met. If they are not the acceptance rates to be derived next may yield wrong results!

#### 1.4.1 Colloid Removal

The acceptance rate for the removal of a colloidal particle is derived first. This is the MC move shown in Fig.1.5. Assume that we start in a state containing  $N_c$  colloids,  $N_p$  polymers and energy  $E$ . It is convenient to label the state as  $(N_c; N_p; E)$ . The energy  $E$  will of course be zero but for the derivation it is convenient to write it down explicitly. After removing the colloid,  $n_p$  polymers are inserted into the depletion zone left behind. The state that we end up in can thus be labeled as  $(N_c - 1; N_p + n_p; E)$ . Note that  $E$  need not be zero: if a second colloid happens to be very close to the colloid that was removed, it could now overlap with one or more of the  $n_p$  polymers that were just inserted.

To enforce detailed balance the probabilities that appear in Eq.(1.6) must be written down. We begin with the easy ones  $P(\rightarrow)$  and  $P(\leftarrow)$ . These are simply given by the grand canonical distribution of Eq.(1.4):

$$P(\rightarrow) = C z_c^{N_c} z_p^{N_p} e^{-E}; \quad P(\leftarrow) = C z_c^{N_c - 1} z_p^{N_p + n_p} e^{-E}; \quad (1.7)$$

The probabilities  $g(\rightarrow)$  and  $g(\leftarrow)$  are more complicated. If we are in state the probability of ending up in state is given by the product of the probabilities of the individual steps that were taken in the MC move. After close inspection of Fig.1.5 the following steps can be identified:

1. Selecting a colloid at random. Since state contains  $N_c$  colloids the probability of choosing one particular colloid is  $1/N_c$ .
2. Selecting  $n_p$ . Since  $n_p$  is drawn uniformly from the interval  $[0; m]$  the probability of this step is  $1/m$ .
3. Selecting  $n_p$  random locations inside a volume  $V$ . The probability of choosing one particular location equals  $1/V$  (see Appendix 1.9). Since  $n_p$  locations are selected we must raise this probability to the power  $n_p$ . Additionally, we pick up a factorial counting the number of ways in which the locations can be selected. The total probability of this step thus becomes  $(n_p)! V^{-n_p}$ .

The probability  $g(\rightarrow)$  is thus the product of the above three terms.

Finally, we derive  $g(\leftarrow)$ . This is the probability that the reverse MC move brings us back from state to state. This move is illustrated in Fig.1.4 and upon inspecting it we observe that state is regenerated if a colloid is placed inside  $V$  at precisely the same location it was just removed from. This carries a probability  $1/V$  and so we find  $g(\leftarrow) = 1/V$ .

Substitution of the above terms into Eq.(1.6) and using the Metropolis choice [8] we find that the removal of a colloid must be accepted with probability:

$$A(N_c \rightarrow N_c - 1) = \min \left[ 1; \frac{m N_c (z_p V)^{n_p}}{z_c V (n_p)!} e^{-(E - E')} \right]; \quad (1.8)$$

Note that moves leading to configurations where  $E$  is not zero are automatically rejected by the above equation.

#### 1.4.2 Colloid Insertion

To make the algorithm complete the acceptance rate for the insertion of a colloid must still be derived, i.e. the MC move of Fig.1.4. We can follow the same reasoning as before with perhaps one subtlety. We start again in a state containing  $N_c$  colloids,  $N_p$  polymers and energy  $E$ , so with label  $(N_c; N_p; E)$ . All polymers (say  $n_p$  of them) that overlap with the inserted colloid are removed, so the state that we end up in can be labeled as  $(N_c + 1; N_p - n_p; E)$ . Again, the energy  $E$  need not be zero: if we are unlucky the inserted colloid overlaps with one or more of the  $N_c$  colloids already present. According to Eq.(1.2) such overlaps also carry infinite energy.

To construct detailed balance we first write down  $P(\rightarrow)$  and  $P(\leftarrow)$ :

$$P(\rightarrow) = C z_c^{N_c} z_p^{N_p} e^{-E}; \quad P(\leftarrow) = C z_c^{N_c+1} z_p^{N_p-n_p} e^{-E}; \quad (1.9)$$

Next, we derive  $g(\rightarrow)$  which is the probability that the MC move of Fig.1.4 generates state starting in state . This involves only the random selection of a location inside  $V$  so we obtain:  $g(\rightarrow) = 1/V$ .

Finally, we consider  $g(\leftarrow)$ . This is the probability that the reverse MC move of Fig.1.5 transforms state back into state . This will happen only if the following conditions are met:

1. The newly inserted colloid is removed again. Since state contains  $N_c + 1$  colloids the probability of this step equals  $1/(N_c + 1)$ .
2. Precisely the same number  $n_p$  of polymers that were removed are inserted again. This step requires some care. Assume that we chose  $m$  rather than  $n$  in Eq.(1.5). In that case the forward move of Fig.1.4 might remove more polymers than the reverse move of Fig.1.5 can possibly put back. This will happen if  $n_p < m$ . Therefore, the probability  $p$  that exactly the same number of polymers are inserted must be written as:

$$p = \begin{cases} 0 & \text{if } n_p < m \\ 1/m & \text{otherwise.} \end{cases} \quad (1.10)$$

3. Selecting the same  $n_p$  coordinates inside  $V$ . As was explained before this probability equals  $(n_p)!/V^{n_p}$ .

The probability  $g(\leftarrow)$  is thus the product of the above three terms.

Substitution into Eq.(1.6) and using the Metropolis choice [8] we find that the insertion of a colloid must be accepted with probability:

$$A(N_c \rightarrow N_c + 1) = \begin{cases} 0 & \text{if } n_p < m \\ \frac{1}{m} \frac{z_c V}{(N_c + 1)} \frac{(n_p)!}{(z_p V)^{n_p}} e^{-(E - E')} & \text{otherwise.} \end{cases} \quad (1.11)$$

Again, moves leading to configurations where  $E$  is not zero are automatically rejected by the above equation.



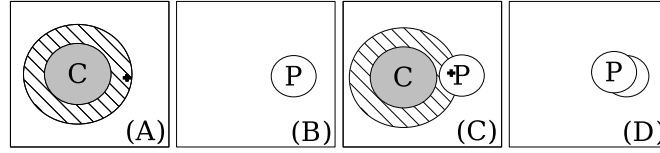


Fig.1.6. Even low values of  $m$  may yield high polymer densities. (A) The starting configuration showing a colloid with its depletion zone. The colloid is removed and one polymer is inserted at a random location inside the depletion zone (cross) resulting in configuration (B). (C) Another colloid is inserted close to the polymer. (D) The colloid is removed again with one polymer inserted in its depletion zone at the cross resulting in two overlapping polymers.

### 1.5 Ergodicity

Now that the MC scheme obeys detailed balance we need to check if it is ergodic. An algorithm is ergodic if every point in phase space can be reached with finite probability. It is easy to see that the algorithm is ergodic as far as the colloids are concerned. For every inserted colloid, a random location inside  $V$  was selected so the entire volume is correctly sampled. Similarly, polymers also sample the entire volume but do so indirectly, namely via the removal of colloids. Whenever a colloid is removed, a number of polymers are inserted in the depletion zone. Since the colloids sample the entire volume, so then do the polymers.

One might argue that the choice of  $m$  in Eq.(1.5) violates ergodicity. If at most  $m - 1$  polymers are inserted for every colloid, the polymer density will always be less than  $(m - 1)/V$  as a result. While this objection sounds reasonable it is in fact unjustified as Fig.1.6 shows.

Fig.1.6 shows an example simulation of the AO model using the cluster algorithm just described with a low value of  $m$ , namely  $m = 2$ . This means that for every removed colloid, at most one polymer is inserted. The starting configuration is a volume containing one colloid, see Fig.1.6A. The edge of the depletion zone of the colloid is also drawn. In Fig.1.6B the colloid is removed and one polymer is placed very close to the edge of the depletion zone (but still inside of it, of course). The simulation is continued in Fig.1.6C where another colloid is placed into the system. This colloid is placed close to the polymer already present, but not too close so the polymer survives. Finally, in Fig.1.6D the colloid is removed again and one polymer is placed inside the depletion zone of this colloid, close to the other polymer. The configuration in Fig.1.6D now shows two polymers practically stacked on top of each other, even though the algorithm was run with  $m = 2$ . This removes the above objection.

Running the algorithm with such a low value of  $m$  is not recommended though. The whole point of this discussion is to show that  $m$  does not influence the correctness of the algorithm, only its efficiency.

## 1.6 Early Rejection Scheme

In Section 1.3 it was argued that the number of polymers  $n_p$  that one needs to insert for every colloid that is removed cannot simply be a constant. In fact, it was shown that  $n_p$  is a random variable described by a Poisson distribution. Yet, in the subsequent description of the algorithm it was decided to draw  $n_p$  uniformly, and not from a Poisson distribution. One might wonder if the efficiency of the algorithm is not seriously impeded by this choice. The answer is it is not, provided one implements the so-called early rejection scheme.

In many MC simulations, the usual approach is to make a change to the system, calculate the involved energy change, select a random number between zero and one, compare this random number to the acceptance rate and finally accept or reject the move. In some cases, particularly in systems where the interactions are hard sphere like, one can do much better.

Consider for example the removal of a colloidal particle displayed in Fig. 1.5 and the associated acceptance rate Eq. (1.8). Most of the quantities appearing in Eq. (1.8) are already known at the start of the move. For example  $N_c$ ,  $V$ ,  $E$ ,  $m$ , and the fugacities. In fact, the only unknowns are  $n_p$  and  $E$ . We also know that if the move is ever going to be accepted  $E$  will be zero at the end. So the only remaining unknown is  $n_p$  which, if you recall, is a random number drawn from the interval  $n_p \in [0; m]$ . The early rejection scheme proceeds as follows:

1. Select a random number  $r$  between zero and one.
2. Select  $n_p$  uniformly from the interval  $n_p \in [0; m]$ .
3. Calculate the acceptance rate  $A(N_c \rightarrow N_c - 1)$  using Eq. (1.8) with the above value for  $n_p$  and assuming that  $E$  is zero.
4. If  $r > A(N_c \rightarrow N_c - 1)$  reject the move immediately otherwise proceed to the next step.
5. Remove the colloid and insert the  $n_p$  polymers. If any of the inserted polymers produce overlap with other colloids reject the move, otherwise the move is accepted.

The most CPU time consuming step in the above scheme is step five. However, this step is only performed for those values of  $n_p$  that are reasonable. Unreasonable values for  $n_p$  were already filtered out in step four at the cost of only a few multiplications and selecting two random numbers. In this scheme it therefore does not matter so much what distribution  $n_p$  is drawn from. Needless to say, the early rejection scheme is highly recommended. To speed up the determination of overlap the link-cell method should also be used.

## 1.7 Application

In this section the grand canonical cluster scheme will be used to study bulk phase separation in the AO model. Since the AO energy is either zero or

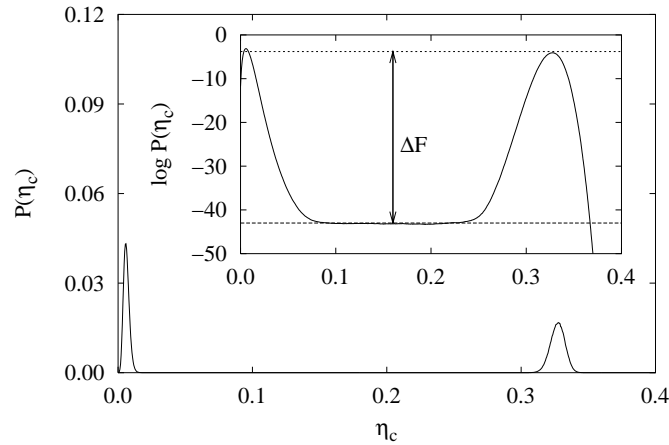


Fig.1.7. Probability  $P(\eta_c)$  of observing a colloid packing fraction  $\eta_c$  for an AO mixture with  $f_q = 0.8$ ;  $z_c = 87.2$ ;  $r_p = 1.0g$  in a simulation of dimensions  $L_x = L_y = 16.7$  and  $L_z = 33.4$ . The probability is not normalized. The inset shows the logarithm of the probability distribution.

in nity the temperature plays no role so we simply put  $\beta = 1$  in the acceptance rates. The phase behavior of the AO model is thus fixed by the colloid to polymer size ratio  $q = R_p/R_c$  and the fugacities  $fz_c; z_p g$ . We consider here a size ratio  $q = 0.8$  and put  $R_c = 1$  to set the length scale. The simulations are performed in a box with edges  $L_x, L_y, L_z$  and using periodic boundary conditions. Following convention we define  $r_p = z_p (4\pi/3)R_p^3$  known as the polymer reservoir packing fraction. Note that  $r_p$  has no relation to the number of polymers actually in the system. It is just a different way of expressing the polymer fugacity  $z_p$ .

In a naive implementation of the scheme one sets the fugacities  $fz_c; r_p g$  and starts the simulation. As the simulation proceeds colloids and polymers will enter and leave the box. The crucial quantity to measure is  $P(\eta_c)$  defined as the probability of observing a box with colloid packing fraction  $\eta_c = (4\pi/3)R_c^3 N_c/V$ . During the simulation one thus maintains a histogram counting how often a certain colloid packing fraction has occurred.

If phase separation occurs  $P(\eta_c)$  is bimodal. An example distribution is shown in Fig.1.7. The peak at low  $\eta_c$  corresponds to the colloid vapor phase (V), the peak at high  $\eta_c$  to the colloid liquid phase (L) and the region in between is the phase-separated regime. The distribution in Fig.1.7 is at coexistence which means that the area under both peaks is equal. At coexistence, the simulation spends equal time in both phases on average. Also shown is the logarithm of  $P(\eta_c)$ . The physical significance of this curve is its relation to the free energy. The height of the barrier marked  $\Delta F$  corresponds to the

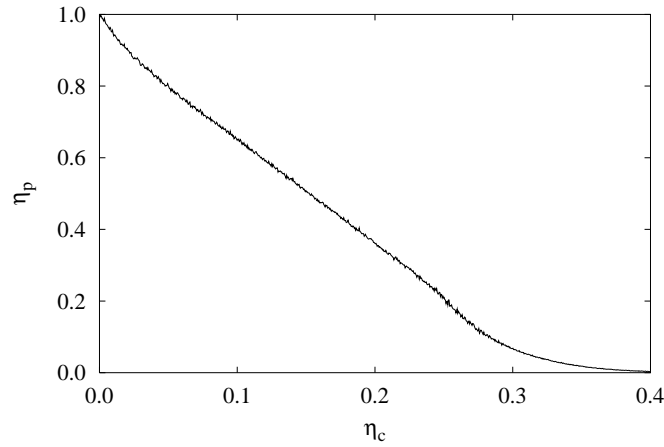


Fig. 1.8. Average polymer packing fraction  $\eta_p$  as a function of the colloid packing fraction  $\eta_c$  for an AO mixture at coexistence with  $q = 0.8$  and  $r_p = 1.0$ .

free energy barrier separating the phases. As was shown by Binder [11] this barrier is related to the surface tension via  $\Delta F = (2A)\gamma$  with  $A$  the area of the interface.

It is also interesting to measure the average polymer packing fraction  $\eta_p$  ( $4\pi R_p^3 N_p / 3V$ ) as a function of  $\eta_c$ . This result is shown in Fig. 1.8. In the pure polymer phase ( $\eta_c = 0$ ) we expect  $\eta_p = r_p$  because the polymers then mimic the ideal gas. This is precisely what Fig. 1.8 shows. As the colloid packing fraction increases the polymer packing fraction in the system decreases to zero.

In the AO model  $r_p$  is the control parameter, much like temperature is for fluid-vapor transitions. To obtain the phase diagram one simply has to measure  $P(\eta_c)$  at coexistence for a number of different  $r_p$ . The problem in a simulation is finding the value of  $\eta_c$  that yields coexistence for the chosen  $r_p$  of interest. Additionally, if the barrier  $\Delta F$  is high, it will be difficult to sample  $P(\eta_c)$  in the region between the peaks. Fortunately, an array of techniques is available to overcome these problems [12]. The results in this work were obtained using a new technique called Successive Umbrella Sampling [13].

For each  $P(\eta_c)$  at coexistence one reads off the colloid packing fraction of the vapor phase  $\eta_c^V$  and of the liquid phase  $\eta_c^L$  and plots the two points  $(\eta_c^V; r_p)$  and  $(\eta_c^L; r_p)$  in a graph. This yields the phase diagram in reservoir representation shown in the inset of Fig. 1.9. By using Fig. 1.8 we can convert the reservoir representation into the experimentally more relevant  $f_c; \phi_g$  or system representation also shown in Fig. 1.9. For every  $P(\eta_c)$  one also obtains a value for the surface tension using the method of Binder. The results of this procedure are shown in Fig. 1.10, in two different representations.

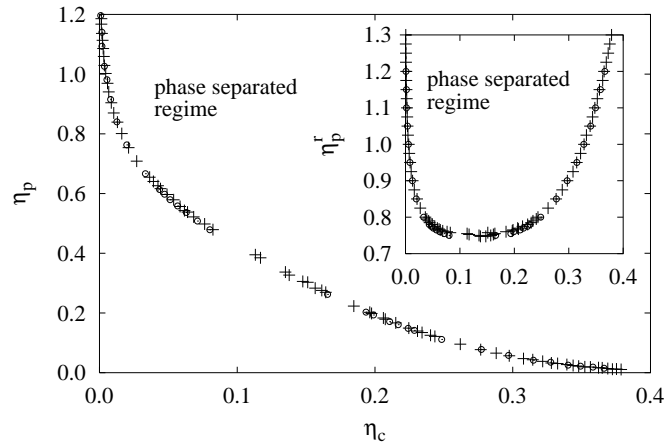


Fig.1.9. Phase diagram of the AO model with  $q = 0.8$  in system representation. Crosses were obtained using box dimensions  $L_x = L_y = 16.7$  and  $L_z = 33.4$ ; open circles were obtained in a smaller box with dimensions  $L_x = L_y = 13.3$  and  $L_z = 26.5$ . The inset shows the phase diagram in reservoir representation.

Finally, we determine the critical polymer fugacity defined as the value of  $\bar{r}_p$  above which phase separation begins to take place. From the inset of Fig.1.9 we see that the critical fugacity is around  $\bar{r}_p = 0.75$ . We have performed a finite size scaling analysis [14] by measuring the cumulant ratio:

$$M = \frac{h(\eta_c - \eta_{ci})^2 i}{h j_c - h_{ci} j^2}; \quad (1.12)$$

as a function of  $\bar{r}_p$  close to the critical point for different system sizes. The results are shown in Fig.1.11. The critical fugacity is at the intersection of the lines from which we obtain  $\bar{r}_{p;cr} = 0.766 \pm 0.002$ .

## 1.8 Conclusions

The grand canonical cluster scheme described in this chapter is very successful at modeling phase separation in AO mixtures. In fact, at the time of writing, it is unsurpassed in speed and accuracy by other simulation methods [15]. However, the method does have its limitations. If the packing fraction of the colloids is high (say 0.40 and above) the algorithm is no longer efficient. In that case the insertion of colloidal particles fails, not because of overlap with polymers, but because of overlap with other colloids. This problem is well known in hard sphere simulations.

The algorithm could be improved for systems where the polymer-polymer interaction is not zero. In these cases the random insertion of  $n_p$  polymers

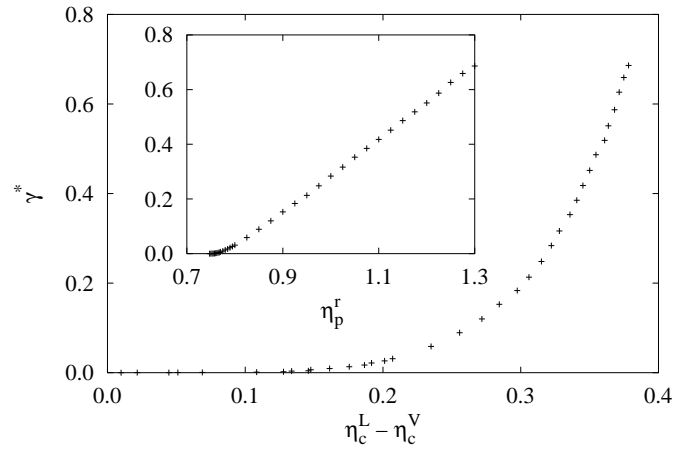


Fig.1.10. Reduced surface tension  $\gamma^*$  for an AO mixture with  $q = 0.8$  as a function of the difference in the colloid packing fractions in the coexisting liquid and vapor phases. The box dimensions were  $L_x = L_y = 16.7$  and  $L_z = 33.4$ . The inset shows  $\gamma^*$  as a function of  $\eta_p^r$ .

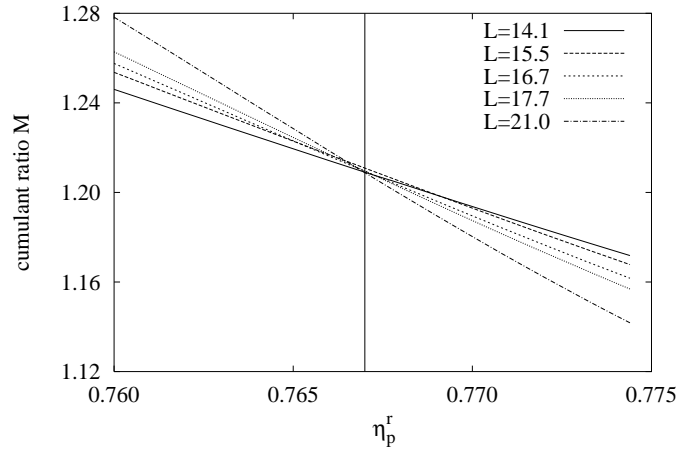


Fig.1.11. Cumulant ratio  $M$  given by Eq.(1.12) as a function of  $\eta_p^r$  for an AO mixture with  $q = 0.8$  for various system sizes. The simulations were performed in a cubic box with edge  $L$  as indicated. From the intercept (vertical line) we obtain for the critical polymer fugacity  $\eta_{p,cr}^r = 0.766 \pm 0.002$ .

into the depletion zone of a colloid may no longer be efficient. Fortunately, the algorithm is easily adapted to include smarter insertion moves such as configurational bias [16], recoil growth [17], worm hole MC [18] and perhaps PERM [19]. Work along these lines is in progress.

Note also that the presented method is general. The derivation of detailed balance for example can easily be modified to an AO model confined between walls or to systems interacting with smooth potentials. This would be the subject of further work.

Acknowledgments I am grateful to the Deutsche Forschungsgemeinschaft for support (TR 6/A 5) and to J. Horbach, K. Binder, M. Müller, M. Schmidt and P. Vimala for collaboration and discussion.

## 1.9 Appendix: Random Points

Here we argue that the selection of a random point inside a volume  $V$  carries a probability  $1/V$ . The question is most easily answered by assuming that the volume is made up of many tiny cells, each with a volume  $\Delta V$ . The total number of cells in the volume is thus equal to  $n = V/\Delta V$  and the probability of picking one of them is  $1/n = \Delta V/V$ .

The difficulty lies in choosing  $\Delta V$ . In statistical mechanics it is assumed that the smallest element of phase space has a volume determined by the thermal wavelength leading to  $\Delta V = \lambda^3$ . This explains why the acceptance rates of grand canonical MC schemes often contain the thermal wavelength [9, 10]. Unfortunately, in a MC simulation this is not very useful. Since the thermal wavelength depends on temperature, particle mass and even the Planck constant, this choice suggests that a simulation of for example hard spheres is temperature and mass dependent.

The key observation is that the physics of the system is indifferent to the choice of  $\Delta V$ . To see this consider Eq.(1.8) which is the acceptance rate for the removal of a colloidal particle. Strictly speaking, the volumes  $V$  and  $V'$  appearing in Eq.(1.8) must be replaced by  $V/\Delta V$  and  $V'/\Delta V$ , respectively. These additional factors of  $\Delta V$  are, however, readily absorbed into the fugacities  $z_c$  and  $z_p$ . The fugacity is given by  $z = \exp(\beta\mu)$  with  $\mu$  the chemical potential, so a rescaling of the fugacity merely shifts  $\mu$  by a constant. This constant has no physical consequence because it in turn shifts the Hamiltonian by a constant. Thus,  $\Delta V$  has no physical consequence and may therefore be set to unity which was done throughout this text.

## References

1. S. Asakura and F. Osawa, J. Chem. Phys. 22, 1255 (1954).
2. A. Vrij, Pure Appl. Chem. 48, 471 (1976).

3. D.G.A.L. Arts, R. Tuinier, and H.N.W. Lekkerkerker, *J. Phys.: Condens. Matter* 14, 7551 (2002).
4. R. Roth, R. Evans, and S. Dietrich, *Phys. Rev. E* 62, 5360 (2000).
5. M. Schmidt, H. Lowen, J.M. Brader, and R. Evans, *Phys. Rev. Lett.* 85, 1934 (2000).
6. M. Dijkstra and R. van Roij, *Phys. Rev. Lett.* 89, 208303 (2002).
7. P. Bolhuis, A. Louis, and J. Hansen, *Phys. Rev. Lett.* 89, 128302 (2002).
8. M.E.J. Newman and G.T. Barkema, *Monte Carlo Methods in Statistical Physics* (Clarendon Press, Oxford, 1999).
9. D.P. Landau and K. Binder, *A Guide to Monte Carlo Simulations in Statistical Physics* (Cambridge University Press, Cambridge, 2000).
10. D. Frenkel and B. Smith, *Understanding Molecular Simulation* (Academic Press, New York, 2000).
11. K. Binder, *Phys. Rev. A* 25, 1699 (1982).
12. N. Widing, *Am. J. Phys.* 69, 1147 (2001).
13. P. Vimala and M. Müller, submitted (2003), preprint cond-mat/0306678.
14. See for example, N. Widing, *Annual Reviews of Computational Physics IV*, page 37 (1996).
15. R.L.C. Vink and J. Horbach, submitted (2003), preprint cond-mat/0310404.
16. J. Siepmann and D. Frenkel, *Mol. Phys.* 75, 59 (1992).
17. S. Consta, N.B. Widing, D. Frenkel, and Z. Alexandrowicz, *J. Chem. Phys.* 110, 3220 (1999).
18. J. Houdayer, *J. Chem. Phys.* 116, 1983 (2002).
19. H. Hsu, V. Mehra, W. Nadler, and P. Grassberger, *J. Chem. Phys.* 118, 444 (2003).